Available online at www.sciencedirect.com
SCIENCE DIRECT®
Polyhedron 23 (2004) 1819–1827
POLYHEDRON
www.elsevier.com/locate/poly

X-ray and electronic structure of the $[ReCl_3(pzH)_2(PPh_3)]$ and $[ReCl_3(3,5\text{-}Me_2pzH)_2(PPh_3)]$ complexes

Barbara Machura [a,*], M. Jaworska [b], Rafal Kruszynski [c,1]

[a] Department of Inorganic and Radiation Chemistry, Institute of Chemistry, University of Silesia, 9th Szkolna St., 40-006 Katowice, Poland
[b] Department of Theoretical Chemistry, Institute of Chemistry, University of Silesia, 9th Szkolna St., 40-006 Katowice, Poland
[c] Department of X-ray Crystallography and Crystal Chemistry, Institute of General and Ecological Chemistry, Łódź University of Technology, 116 Żeromski St., 90-924 Łódź, Poland

Received 17 March 2004; accepted 13 April 2004
Available online 18 May 2004

Abstract

X-ray structures of new $[ReCl_3(pzH)_2(PPh_3)]$ and $[ReCl_3(3,5\text{-}Me_2pzH)_2(PPh_3)]$ complexes (pzH = pyrazole) have been determined, and the geometric parameters of $[ReCl_3(pzH)_2(PPh_3)]$ have been examined using density functional theory (DFT) method. The UV–Vis spectra of the complexes have been discussed on the basis of the electronic transitions of $[ReCl_3(pzH)_2(PPh_3)]$ calculated with time-dependent DFT method (TDDFT).

Keywords: Rhenium complexes; Pyrazole ligand; X-ray structure; DFT calculations

1. Introduction

The noticeable growth of interest in the rhenium coordination chemistry is connected with the favourable nuclear properties of ^{186}Re and ^{188}Re nuclides, which make the radioisotopes useful for diagnostic nuclear medicine and applications in radioimmunotherapy [1,2]. Although pyrazole and its derivatives have a special place among N-donor ligands, the number of rhenium complexes containing these ligands is limited [2–6].

Previously, we investigated the reactivity of oxorhenium(V) species – $[ReO(OEt)X_2(PPh_3)_2]$, $[ReOX_3(PPh_3)_2]$ and $[ReOX_3(AsPh_3)(OAsPh_3)]$ (X = Cl or Br) – towards pyrazole (pzH) and 3,5-dimethylopyrazole (3,5-Me_2pzH) under various reaction conditions. The products of these syntheses include: (i) mononuclear $[ReOX_2\{\eta^2\text{-}N_2C_3H_3C(CH_3)_2O\}(PPh_3)]$ complexes with $C_3H_3N_2C(CH_3)_2O^-$ anion obtained in the addition reaction of pyrazole and acetone and (ii) dinuclear Re(V) compounds of types $[\{Re(O)X(PPh_3)\}_2(\mu\text{-}O)(\mu\text{-}pz)_2]$, $[\{Re(O)X_2(3,5\text{-}Me_2pzH)_2\}_2(\mu\text{-}O)]$, $[\{Re(O)Br(3,5\text{-}Me_2pzH)\}_2(\mu\text{-}O)(\mu\text{-}3,5\text{-}Me_2pz)_2]$, $[\{Re(O)X(PPh_3)\}_2(\mu\text{-}O)(\mu\text{-}3,5\text{-}Me_2pz)_2]$ and $[\{Re(O)X(PPh_3)\}(\mu\text{-}O)(\mu\text{-}3,5\text{-}Me_2pz)_2\{Re(O)X(3,5\text{-}Me_2pzH)\}]$ (X = Cl or Br) [7,8].

Here, we report the synthesis and X-ray structure of the two mononuclear Re(III) $[ReCl_3(pzH)_2(PPh_3)]$ (**1**) and $[ReCl_3(3,5\text{-}Me_2pzH)_2(PPh_3)]$ (**2**) complexes and the results of the density functional theory (DFT) calculations for **1**. The UV–Vis spectra of **1** and **2** are discussed basing on the electronic transitions of **1**, calculated using the time-dependent DFT method (TDDFT).

2. Experimental

2.1. General procedure

The reactions were carried out under argon atmosphere. All solvents were of reagent grade and were used as received. Ammonium perrhenate, Ph_3P and pyrazole (pzH) were purchased from Aldrich and used as

* Corresponding author. Tel.: +48322582441; fax: +48322599978.
E-mail addresses: basia@tc3.us.ich.edu.pl (B. Machura), mj@tc3.i-ch.us.edu.pl (M. Jaworska).
[1] A holder of the Foundation for Polish Science (FNP) scholarship.

0277-5387/$ - see front matter © 2004 Elsevier Ltd. All rights reserved.
doi:10.1016/j.poly.2004.04.017

received. $[Re(MeCN)Cl_3(PPh_3)_2]$ and $[ReOCl_3(PPh_3)_2]$ complexes and 3,5-Me_2pzH were prepared according to the literature methods [9–11].

IR spectra were recorded on a Nicolet Magna 560 spectrophotometer in the spectral range 4000–400 cm^{-1} with the samples in the form of KBr pellets. Electronic spectra were measured on a spectrophotometer Lab Alliance UV–Vis 8500 in the range 800–220 nm in deoxygenated dichloromethane solution. The magnetic susceptibility was determined with a superconducting quantum interference device (SQUID, Quantum Design) magnetometer. Elemental analyses (C, H and N) were performed on a Perkin–Elmer CHN-2400 analyser.

2.2. Preparation of $[ReCl_3(pzH)_2(PPh_3)]$ (**1**)

2.2.1. Method A (**1a**)

$[ReOCl_3(PPh_3)_2]$ (1 g, 1.20 mmol) and pzH (0.54 g, 8 mmol) in diisopropyl ketone (60 cm^3) were refluxed for 2 h. The starting material gradually dissolved and the colour of the reaction solution changed from green to dark brown. The volume of the reaction solution was condensed to 20 cm^3 and reddish-orange microcrystalline solid was formed by an addition of 100 cm^3 of diethyl ether. The product was washed with EtOH and cold ether, and dried in vacuo.

2.2.2. Method B (**1b**)

$[Re(MeCN)Cl_3(PPh_3)_2]$ (1 g, 1.20 mmol) and pzH (0.54 g, 8 mmol) in chloroform (80 cm^3) were refluxed for 4 h. The starting material gradually dissolved and the colour of the reaction solution became dark red. After 3 h, the reddish-orange microcrystalline solid started to participate. The volume was condensed to 10 cm^3, diethyl ether (100 cm^3) was added and reddish-orange microcrystalline solid was filtered. The product was washed with EtOH and cold ether, and dried in vacuo.

The crystals of **1a** and **1b** suitable for X-ray investigation were obtained by recrystallization from a mixture of acetonitrile and dichloromethane (yield 80%).

The solvents used for the reactions and recrystallization were not dried, so some water was present in the reaction systems and water molecule was found in **1b** structure.

IR(KBr, cm^{-1}) 3154 (s), 3134 (m) 3115 (w), 2939 (m), 2903 (m), 2840 (m), 2810 (w), 1610 (w) 1572 (w), 1497 (w), 1479 (m), 1458 (m), 1435 (s), 1400 (s), 1346 (w), 1317 (m), 1256 (m) 1192 (w), 1126 (s), 1093 (s), 1068 (w), 1050 (m), 1042 (s), 999 (w), 955 (w), 906 (w), 854 (w), 788 (m), 768 (m), 746 (s), 698 (s), 689 (s), 609 (w), 598 (w), 526 (s), 510 (s), 495 (m), 449 (w), 432 (w). Anal. Calc for $C_{24}H_{23}N_4Cl_3PRe$: C, 41.72; H, 3.35; N, 8.11. Found: C, 41.98; H, 3.56; N, 8.20%.

2.3. Preparation of $[ReCl_3(3,5\text{-}Me_2pzH)_2(PPh_3)]$ (**2**)

$[Re(MeCN)Cl_3(PPh_3)_2]$ (1 g, 1.20 mmol) and 3,5-Me_2pzH (0.77 g, 8 mmol) in chloroform (80 cm^3) were refluxed for 4 h. The starting material gradually dissolved and the colour of the reaction solution became dark red. After 3 h, the reddish-orange microcrystalline solid started to participate. The volume was condensed to 10 cm^3, diethyl ether (100 cm^3) was added and reddish-orange microcrystalline solid was filtered. The product was washed with EtOH and cold ether, and dried in vacuo. The crystals of **2** suitable for X-ray investigation were obtained by recrystallization from a mixture of acetonitrile and dichloromethane (yield 85%).

IR(KBr, cm^{-1}) 3384 (s), 3354 (s) 3138 (w), 3055 (m), 2922 (m), 1567 (s) 1482 (m), 1465 (w), 1432 (s), 1395 (m), 1372 (m), 1275 (s) 1177 (m), 1149 (m), 1091 (s), 1031 (s), 999 (w), 813 (w), 800 (m), 744 (s), 694 (s), 650 (m), 644 (m), 555 (w), 524 (s), 511 (s), 497 (s), 448 (m). *Anal.* Calc. for $C_{28}H_{31}N_4Cl_3PRe$: C, 45.01; H, 4.18; N, 7.50. Found: C, 45.33; H, 4.29; N, 7.60%.

2.4. Crystal structures determination and refinement

The X-ray intensity data were collected on a KM-4-CCD automatic diffractometer equipped with CCD detector with 24, 32 and 40 s exposure time (for compounds **1a**, **1b** and **2**, respectively) was used and the whole Ewald sphere (up to $2\theta = 50°$) was collected. The unit cell parameters were determined from least-squares refinement of the setting angles of 8345°, 6543° and 5421° (respectively, as above) of strongest reflections. Details concerning crystal data and refinement are given in Table 1. Lorentz, polarization and numerical absorption corrections [12] were applied. The structures was solved by the Patterson method and subsequently completed by the difference Fourier recycling. All the non-hydrogen atoms were refined anisotropically using full-matrix, least-squares technique. The hydrogen atoms of the phenyl rings were treated as ''riding'' on their parent carbon atoms [d(C–H) = 0.96 Å] and assigned isotropic temperature factors equal 1.2 times the value of equivalent temperature factor of the parent carbon atom. SHELXS 97 [13], SHELXL 97 [14] and SHELXTL [15] programs were used for all the calculations. Atomic scattering factors were those incorporated in the computer programs.

The crystals of **1a** have the diffused electron density originated from multipositional disordered solvent water molecule around special position 0, 1/2 and 1/2. This effect was repeatable for all measured crystals in the sample. In the crystals of **1b** it can be found slightly dynamically disordered water molecule that is also statically disordered in two symmetry equivalent positions.

The N2/C21 and N4/C24 atoms in structure of **1** were distinguished on the basis of anisotropic parameters. Changing the carbon atoms to nitrogen and vice versa

Table 1
Crystal data and structure refinement for **1a**, **1b** and **2**

	1a	**1b** ($1 \cdot 1/2H_2O$)	**2**
Empirical formula	$C_{24}H_{23}Cl_3N_4PRe$	$C_{24}H_{24}Cl_3N_4O_{0.5}PRe$	$C_{28}H_{31}Cl_3N_4PRe$
Formula weight	690.98	699.99	747.09
Temperature (K)	291(2)	293(2)	293(2)
Wavelength (Å)	0.71073	0.71073	0.71073
Space group	$P2_1/n$	$P2_1/n$	$P\bar{1}$
Crystal system	monoclinic	monoclinic	triclinic
Unit cell dimensions			
a (Å)	11.4910(9)	11.4101(6)	10.2682(8)
b (Å)	17.5839(15)	17.6808(9)	13.0183(15)
c (Å)	13.8284(12)	13.7198(9)	13.0572(14)
α (°)			66.249(11)
β (°)	108.030(7)	107.418(5)	76.127(8)
γ (°)			68.374(9)
Volume (Å^3)	2656.9(4)	2640.9(3)	1476.6(3)
Z	4	4	2
D_{calc} (Mg m^{-3})	1.727	1.761	1.680
Absorption coefficient (mm^{-1})	4.955	4.988	4.465
$F(000)$	1344	1364	736
Crystal size (mm)	$0.69 \times 0.26 \times 0.06$	$0.22 \times 0.11 \times 0.04$	$0.26 \times 0.12 \times 0.10$
θ range for data collection (°)	3.61–25.16	3.08–25.11	3.19–25.10
Index ranges	$-13 \leqslant h \leqslant 13$	$-13 \leqslant h \leqslant 13$	$-12 \leqslant h \leqslant 12$
	$-20 \leqslant k \leqslant 20$	$-21 \leqslant k \leqslant 21$	$-15 \leqslant k \leqslant 15$
	$-16 \leqslant l \leqslant 16$	$-16 \leqslant l \leqslant 16$	$-15 \leqslant l \leqslant 15$
Reflections collected	29 535	27 515	14 778
Independent reflections	4740 ($R_{int} = 0.0691$)	4703 ($R_{int} = 0.0566$)	5249 ($R_{int} = 0.0770$)
Completeness to 2θ (%)	96.0	96.4	99.8
Maximum and minimum transmission	0.769 and 0.130	0.887 and 0.406	0.770 and 359
Data/restraints/parameters	4740/0/298	4703/0/307	5249/0/336
Goodness-of-fit on F^2	1.156	1.096	0.991
Final R indices [$I > 2\sigma(I)$]	$R_1 = 0.0566$	$R_1 = 0.0331$	$R_1 = 0.0293$
	$WR_2 = 0.1453$	$wR_2 = 0.0727$	$wR_2 = 0.0648$
R indices (all data)	$R_1 = 0.0580$	$R_1 = 0.0482$	$R_1 = 0.0353$
	$WR_2 = 0.1465$	$wR_2 = 0.0782$	$wR_2 = 0.0667$
Largest difference peak and hole (e Å^{-3})	2.887 and −1.123	1.029 and −0.791	1.355 and −0.833

1a, data for the **1** complex obtained according to method A.
1b, data for the **1** complex obtained according to method B.

cause anisotropic displacement parameters to be senseless.

2.5. Computational details

GAUSSIAN 03 program [16] was used in the calculations. The geometry optimization was carried out using the DFT method with the use of B3LYP functional [17,18]. The electronic spectrum was calculated with the TDDFT method [19].

LANL2DZ basis set [20] was used on the rhenium atom, 6-31G(d) on the chlorine, nitrogen, phosphorus and carbon atoms and 6-31G basis on the hydrogen atoms in the calculations.

3. Results and discussion

Two different routes have been employed for the preparation of **1**. The refluxing of $[ReOCl_3(PPh_3)_2]$ with pzH in diisopropyl ketone gives the complex **1** in moderate yield. The well-known capacity of PPh_3 to interact with the Re≡O bond in the rhenium(V) oxo-complexes explains the course of the reaction between $[ReOCl_3(PPh_3)_2]$ and pyrazole:

$$2[ReOCl_3(PPh_3)_2] + 2N_2C_3H_4 \rightarrow [ReCl_3(pzH)_2(PPh_3)] + OPPh_3$$

A higher yield of **1** has been reported for the substitution reaction:

$$[ReCl_3(MeCN)(PPh_3)_2] + 2pzH \rightarrow [ReCl_3(pzH)_2(PPh_3)] + MeCN + PPh_3.$$

The complex **2** has been obtained in the reaction of $[ReCl_3(MeCN)(PPh_3)_2]$ with 3,5-Me_2pzH. The excess of pyrazole and 3,5-Me_2pzH used in the reactions ensure the maximum yield of the complexes.

3.1. X-ray structure

A perspective drawings of **1** and **2** are given in Figs. 1 and 2, respectively. The rhenium atom of the both

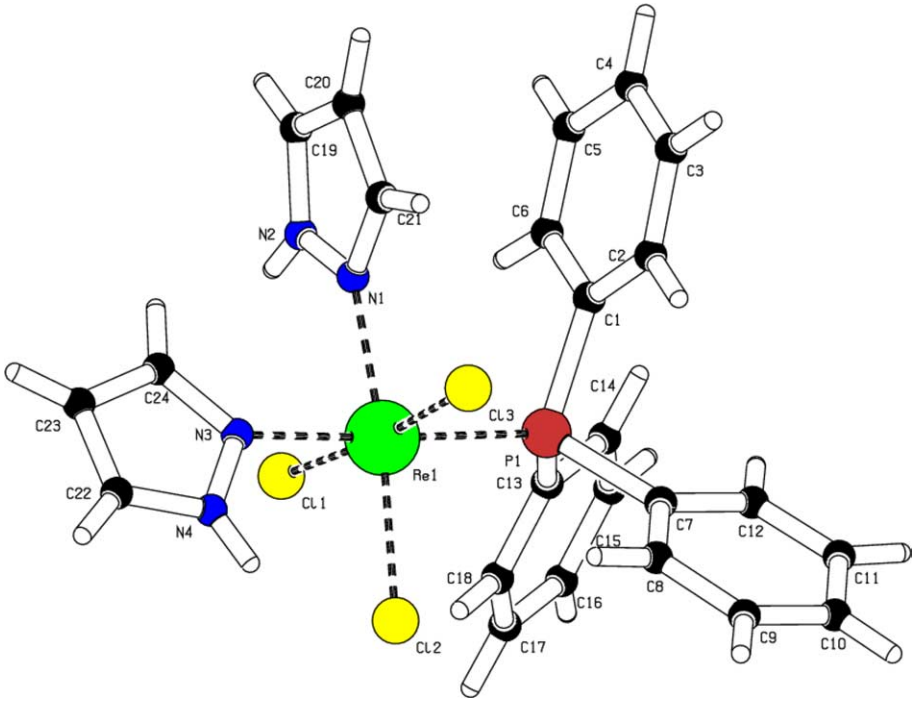

Fig. 1. The molecular structure of **1**.

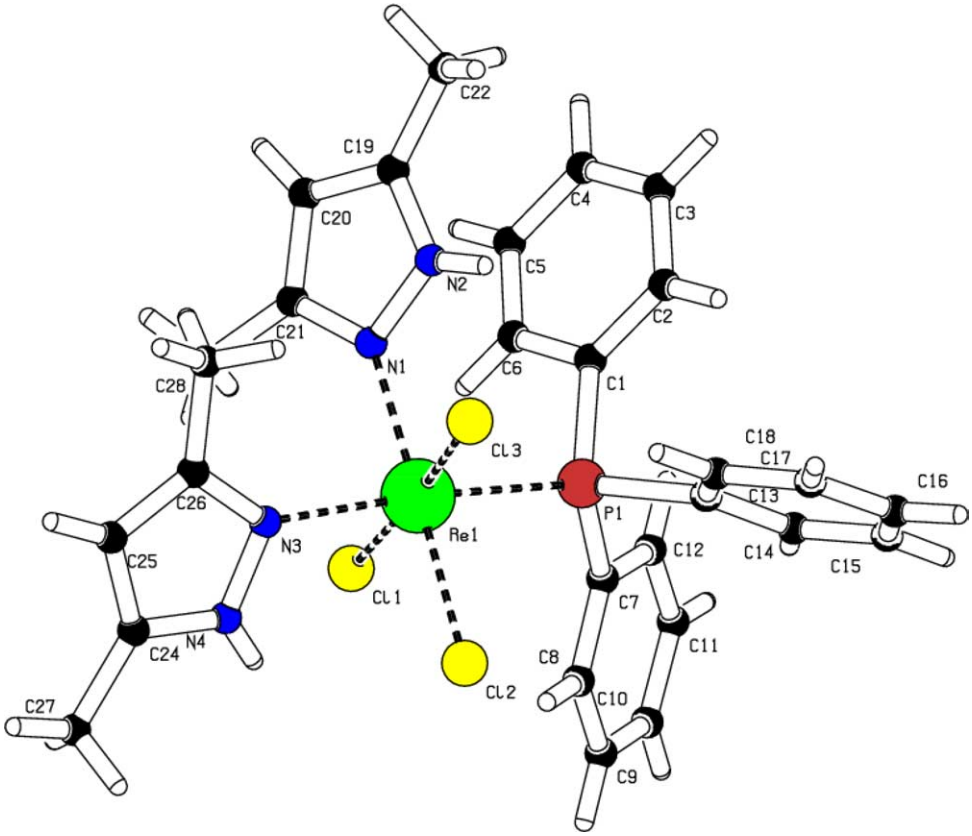

Fig. 2. The molecular structure of **2**.

complexes is in distorted octahedral environment with three chlorine ligands in *mer* geometry, two N-donor ligands (pzH or 3,5-Me_2pzH) in *cis* position to each other and one PPh_3 molecule occupying *trans* position to N(3) atom. Table 1 presents crystal data and structural refinement for **1a**, **1b** and **2**. The most important bond lengths and angles for compounds **1a**, **1b** and **2** are reported in Table 2. A notable *trans* influence of triphenylphosphine ligand is observed in both complexes; the Re–N(3) bond lengths are longer in comparison with the corresponding Re–N(1) distances. The Re–N, Re–Cl and Re–P bond lengths are unexceptional, they agree well with appropriate values found previously in similar rhenium compounds [7,8,21–23].

The weak intramolecular and intermolecular hydrogen bonds [24–26] of **1** and **2** are presented in Table 3.

3.2. Infrared data

The strong bands in the range assignable to N–H vibrations (3400–3100 cm^{-1}) in the IR spectra of **1** and **2** confirm the coordination of pyrazoles ligands in the neutral monodentate form. The characteristic bands of the C=C and C=N stretching modes, observed at 1640 and 1558 cm^{-1} in uncomplexed pyrazole and at 1663 and 1595 cm^{-1} in uncomplexed 3,5-dimethylpyrazole, are shifted to considerable lower frequencies.

3.3. Magnetochemical measurements

Magnetic susceptibilities of **1** were recorded over the temperature range 5–300 K. Temperature dependence of the molar magnetic susceptibility for **1** is presented in Fig. 3. The observed room-temperature effective magnetic moment 1.2 BM is typical of the rhenium(III) mononuclear complexes. It consistent with low-spin rhenium(III) (d^4) ions in O_h field [27] and arises because of the large spin–orbit coupling ($\xi = 2500$ cm^{-1}) [28].

3.4. The optimized geometry and molecular orbitals of *1*

The geometry of **1** was optimized in triplet and singlet states using the DFT method with the B3LYP functional. The energy of the singlet state is of 16.3 kcal higher. The optimized geometric parameters of the triplet state are gathered in Table 2. The optimized geometry of **1** is in good agreement with the experimental one and the largest differences are found for Re–Cl bond distances.

The selected HOMO and LUMO orbitals with α-spin for **1** are depicted in Fig. 4. The following orientation of the axes has been used for determination of the MO characters: the *z*-axis goes along Cl(1)–Re–Cl(3) linkage and *x* goes through the N(3)–Re–P(1) bonds. The rhenium d_π atomic orbital (d_{xz}, d_{yz} and d_{xy}) and π orbitals of chlorine ligands in anti-bonding arrangement make main contributions into the HOMO-2, HOMO-1 and

Table 2
The experimental bond lengths (Å) and angles (°) for **1a**, **1b** and **2** and the optimized bond lengths (Å) and angles (°) for **1**

	Experimental		Optimized	Experimental
	1a	**1b**	**1**	**2**
Bond lengths				
Re(1)–Cl(1)	2.345(2)	2.3452(15)	2.448	2.3713(12)
Re(1)–Cl(2)	2.400(2)	2.3993(15)	2.489	2.3956(11)
Re(1)–Cl(3)	2.357(2)	2.3614(15)	2.407	2.4009(12)
Re(1)–N(1)	2.135(7)	2.127(5)	2.166	2.135(3)
Re(1)–N(3)	2.167(8)	2.194(5)	2.164	2.185(3)
Re(1)–P(1)	2.421(2)	2.4296(14)	2.487	2.4466(11)
Bond angles				
N(1)–Re(1)–N(3)	85.8(3)	85.98(16)	87.13	89.24(12)
N(1)–Re(1)–Cl(1)	87.4(2)	86.75(13)	87.12	92.87(9)
N(3)–Re(1)–Cl(1)	87.1(2)	88.20(12)	88.59	86.70(10)
N(1)–Re(1)–Cl(2)	173.80(19)	173.97(12)	173.88	174.36(9)
N(3)–Re(1)–Cl(2)	88.2(2)	88.48(12)	87.21	87.22(9)
Cl(1)–Re(1)–Cl(2)	90.43(9)	90.71(6)	90.42	91.31(4)
N(1)–Re(1)–Cl(3)	88.7(2)	89.21(13)	87.52	85.92(9)
N(3)–Re(1)–Cl(3)	87.7(2)	87.38(12)	89.43	88.26(10)
Cl(1)–Re(1)–Cl(3)	173.77(9)	174.21(6)	174.37	174.83(4)
Cl(2)–Re(1)–Cl(3)	92.89(9)	92.90(6)	94.75	89.58(4)
N(1)–Re(1)–P(1)	92.03(19)	91.40(12)	93.40	93.47(9)
N(3)–Re(1)–P(1)	177.2(2)	175.94(12)	178.99	172.08(10)
Cl(1)–Re(1)–P(1)	94.67(8)	94.75(5)	92.30	85.73(4)
Cl(2)–Re(1)–P(1)	93.94(8)	94.26(5)	92.30	90.61(4)
Cl(3)–Re(1)–P(1)	90.36(8)	89.49(5)	89.73	99.35(4)

Table 3
Hydrogen bonds for **1a**, **1b** and **2**

D	A	H···A		D···A		D–H···A	
		1a	**1b**	**1a**	**1b**	**1a**	**1b**
N(4)	Cl(2)	2.60	2.57	3.114(8)	3.102(6)	119.8	120.6
N(4)	Cl(2#1)	2.55	2.58	3.225(8)	3.254(6)	135.7	135.5
N(2)	Cl(1)	2.65	2.63	3.148(12)	3.112(7)	117.9	116.8
C(8)	Cl(2)	2.77		3.439(11)		129.8	
C(8)	Cl(3)	2.83		3.507(11)		130.9	
C(21)	Cl(3)	2.58	2.62	3.136(10)	3.159(6)	118.7	117.4
C(14)	Cl(2)		2.74		3.425(6)		131.2
2							
N(2)	Cl(3)	2.71		3.105(4)		111.7	
N(4)	Cl(2)	2.79		3.155(4)		111.5	
C(8)	Cl(2)	2.68		3.526(6)		151.8	
C(18)	Cl(3)	2.54		3.435(6)		160.4	
C(20)	Cl(2#2)	2.81		3.629(5)		147.1	
C(28)	Cl(3)	2.68		3.511(5)		144.9	

#1: $2-x,-y,1-z$ for **1a** and $-x,-y,-z$ for **1b**.
#2: $x-1,y,z$.

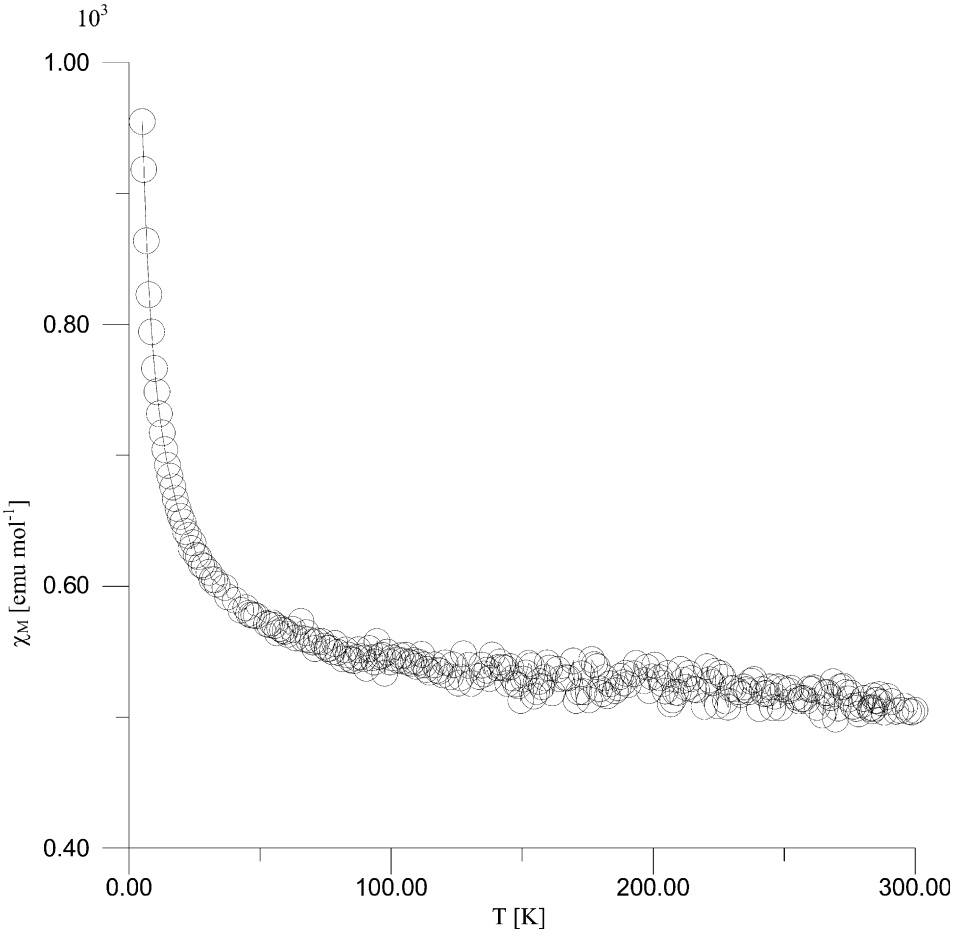

Fig. 3. Temperature dependence of the molar susceptibility for **1**.

HOMO with α-spin and HOMO, LUMO and LUMO + 1 with β-spin. The HOMO orbitals have also the antibonding contribution from the pyrazole ligands. The lower lying orbitals are π orbitals of the phenyl groups and pyrazole ligands. HOMO-11 and HOMO-5 with α-spin and HOMO-9 and HOMO-3 with β-spin

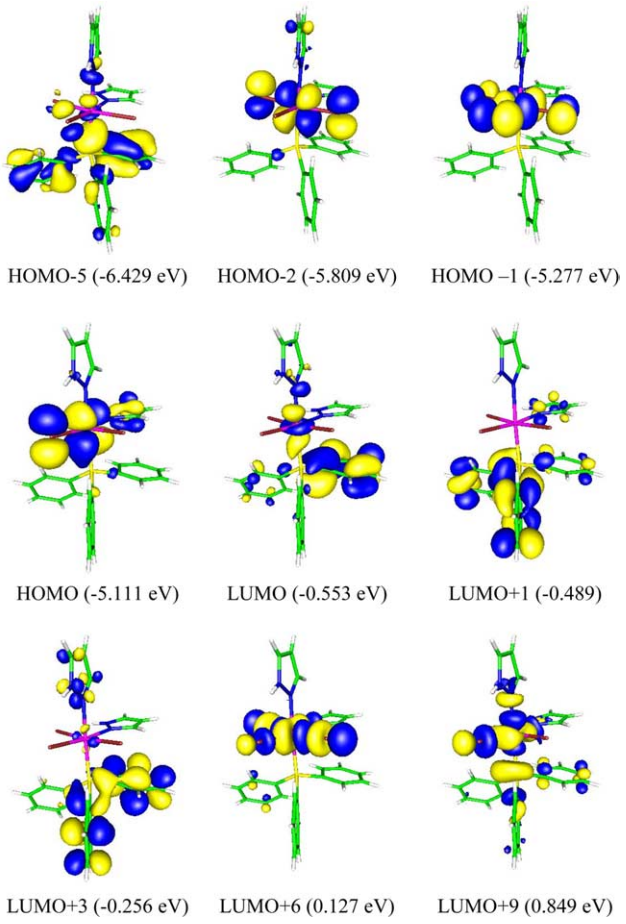

Fig. 4. The selected HOMO and LUMO orbitals with α-spin for **1**.

have a substantial contribution from the free electron pairs on the phosphorus atom. The LUMO+6 with α-spin and the LUMO+10 with β-spin are the antibonding orbital of $d_{z2} - \sigma_{Cl}$ character. The LUMO+9 with α-spin and the LUMO+11 with β-spin are the antibonding orbital of $d_{x^2-y^2} - \sigma_{Cl} - \sigma_N - \sigma_P$ character. LUMO, LUMO + 3 and LUMO + 1 with α-spin, and LUMO+2 and LUMO+3 with β-spin have large participation of p phosphorus orbitals.

3.5. UV–Vis spectra of *1* and *2* and electronic spectrum of *1* from the TDDFT calculations

The complexes under investigation are high spin systems. The calculations with TDDFT method for open-shell organic, inorganic and organometallic molecules are still limited but a few studies have already appeared and supported the TDDFT method to be applicable for such systems giving good assignment of experimental spectra [29–33]. There are also several works performed with this method for 5d-metal (including rhenium complexes) in which good correlations between experimental and calculated results have been confirmed [34–40].

The energy and molar absorption coefficients of experimental absorption bands of **1** and **2** are presented in Table 4. The spin-allowed triplet–triplet electronic transitions of **1** calculated with the TDDFT method are presented in Table 5. Except for the low energy part of the spectrum, only transitions with oscillator strengths larger than 0.01 are listed. The UV–Vis spectrum of **1** was calculated only to 260 nm. Nevertheless, on the basis of the calculated transitions for PPh_3 and [$ReCl_3(pzH)_3$] [41], it can be assumed that the experimental bands of **1** and **2** at energy below 240.0 nm correspond to intraligand $\pi \rightarrow \pi^*$ transitions in phosphine and pyrazole ligands. The solution spectra of pyrazole and PPh_3 exhibit intense absorption band at 231.6 and 217.6 nm, respectively, which can support this assignment.

The assignment of the calculated transitions to the experimental bands was based on the criterion of the energy and oscillator strength of the calculated transition. The long-wave experimental bands are of low intensity and they are compared to the calculated long-wave transitions with small oscillator strengths. The remaining absorption experimental bands are of much higher intensity and they are compared to the calculated transitions with high oscillator strengths.

The longest wave experimental bands of **1** and **2** (at 507.3 and 547.8 nm, respectively) may be attributed to the calculated transitions of $\pi_{Cl} \rightarrow d$ and $\pi_{Ph} \rightarrow d$ character (at 407.4 and 401.0 nm) and $d \rightarrow \pi^*_{Ph}$ character (at 404.5 nm) with small oscillator strengths. The transitions from π_{Ph} to metal d orbitals are mediated by phosphorus.

The next experimental bands of **1** and **2** (at 390.8 and 379.6 nm, respectively) can be assigned to the calculated transitions at 385.5 and 381.4 nm. They have MLCT ($d \rightarrow \pi^*_{pzH}$) character with small contribution of d–d

Table 4
The energy and molar absorption coefficients of experimental absorption bands for **1** and **2**

Band position (nm)	Band position (eV)	ε
1		
507.3	2.44	350
390.8	3.17	1040
331.1	3.74	1620
263.8	4.70	2200
238.0	5.21	3900
200.1	6.20	7200
2		
547.8	2.26	400
379.6	3.27	1220
338.4	3.66	3700
269.0	4.61	5470
229.0	5.41	8910
213.0	5.82	7330

ε, molar absorption coefficient ($dm^3\ mol^{-1}\ cm^{-1}$).

Table 5
The most important electronic transitions calculated with the TDDFT method for **1**

The most important orbital excitations		λ (nm)	E (eV)	f
α-spin	β-spin			
	H-5(π_{Cl}) → L(d)	407.4	3.04	0.0004
	H-2(π_{Ph}) → L(d)			
	H(d_{xy}) → L + 3(π^*_{Ph})	404.5	3.06	0.0028
	H(d_{xy}) → L + 8(π^*_{Ph})			
	H-3 (n_P + π_{Ph}) → L(d)	401.0	3.09	0.0080
	H(d_{xy}) → L + 4(π^*_{pzH})	385.5	3.22	0.0113
H(d_{xy}) → L + 6(d_{z2})	H(d_{xy}) → L + 2(π^*_{Ph})	381.4	3.25	0.0046
	H(d_{xy}) → L + 10(d_{z2})			
	H-1(π_{Ph}) → L(d_{xz})	376.1	3.30	0.0035
	H-4(π_{Ph}) → L(d_{xz})	355.3	3.49	0.0039
H(d_{xy}) → L(π^*_{Ph})		352.7	3.52	0.0033
	H-5(π_{Cl}) → L + 1(d_{yz})	351.2	3.53	0.0194
	H-2(π_{Ph}) → L + 1(d_{yz})			
H(d_{xy}) → L + 1(π^*_{Ph})		314.7	3.94	0.0266
H(d_{xy}) → L + 2(π^*_{pzH})		305.6	4.06	0.0491
	H-10(π_{Cl} + π_{pzH}) → L + 1(d_{yz})	283.7	4.37	0.0217
	H-9(π_{Cl} + π_{pzH} + π_{Ph} + n_p) → L + 1(d_{yz})			
	H-9(π_{Cl} + π_{pzH} + π_{Ph} + n_p) → L + 1(d_{yz})	280.9	4.41	0.0204
	H-6(π_{Ph}) → L + 1(d_{yz})			
H-2(d_{xz}) → L + 3(π^*_{Ph})	H-13(π_{pzH}) → L(d_{xz})	277.0	4.48	0.0253

electronic transitions. Owing to the small oscillator strengths, the three calculated transitions at 376.1, 355.3 and 352.7 nm of π_{Ph} → d and d → π^*_{Ph} character do not contribute significantly to the overall shape of the spectrum. In the experimental spectrum such small transitions are hidden under the more intense ones.

The experimental bands of **1** and **2** at 331.1 and 338.4 nm, respectively, are attributed to the calculated transitions at 351.2, 314.7 and 305.6 nm. The first one is a π_{Cl} → d(LMCT) transition, the two others have d → π^*_{pzH}(MLCT) character.

The absorption bands recorded at 263.8 and 269.0 nm for **1** and **2**, respectively, are assigned to the calculated transitions at 283.7, 280.9 and 277.0 nm with large oscillator strengths. They are of LMCT (π_{pzH} → d, π_{Cl} → d and π_{Ph} → d) character.

The LUMO + 1 and LUMO + 3 with α-spin and LUMO + 2 and LUMO + 3 orbitals with β-spin have a substantial admixture of phosphorus orbitals so the transitions from metal to π^*_{Ph} orbitals are mediated by phosphorus.

4. Supplementary data

Supplementary data are available from the CCDC, 12 Union Road, Cambridge CB2 1EZ, UK (fax: +44-1223-336033; E-mail: deposit@ccdc.cam.ac.uk or www: http://www.ccdc.cam.ac.uk) on request, quoting the deposition numbers: 233906 ($C_{24}H_{23}Cl_3N_4PRe$), 233907 ($C_{24}H_{24}Cl_3N_4O_{0.5}PRe$) and 233908 ($C_{28}H_{31}Cl_3N_4PRe$).

Acknowledgements

The GAUSSIAN 03 calculations were carried out in the WrocŁaw Centre for Networking and Supercomputing, WCSS, WrocŁaw, Poland, under calculational grant No. 51/96.

Crystallographic part was financed by funds allocated by the Ministry of Scientific Research and Information Technology to the Department of X-ray Crystallography and Crystal Chemistry, Institute of General and Ecological Chemistry, Łódź University of Technology.

The authors thank G. Jakob from University of Mainz for magnetic measurement.

References

[1] W. Volkert, W.F. Goeckeler, G.J. Ehrhardt, A.R. Ketring, J. Nucl. Med. 32 (1991) 174.
[2] E.A. Deutsch, K. Libson, J.L. Vanderheyden, Technetium and Rhenium in Chemistry and Nuclear Medicine, Raven Press, New York, 1990.
[3] S. Trofimenko, Chem. Rev. 72 (1972) 497.
[4] S. Trofimenko, Inorg. Chem. 34 (1986) 115.
[5] G. La Monica, G.A. Ardizzoia, Prog. Inorg. Chem. 46 (1997) 151.
[6] G.A. Ardizzoia, G. La Monica, A. Maspero, M. Moret, N. Masciocchi, Eur. J. Inorg. Chem. (1998) 1503.
[7] B. Machura, J.O. Dzięgielewski, S. Michalik, R. Kruszynski, T.J. Bartczak, J. Kusz, Transit. Met. Chem. 28 (2003) 939.
[8] B. Machura, J.O. Dzięgielewski, R. Kruszynski, T.J. Bartczak, J. Kusz, Inorg. Chim. Acta 357 (2004) 1011.
[9] G. Rouschias, G. Wilkinson, J. Chem. Soc. A 465 (1966).
[10] G. Rouschias, G. Wilkinson, J. Chem. Soc. A 993 (1967).
[11] A.I. Vogel, Textbook of Practical Organic Chemistry, Longman Group Limited, New York, 1978.

[12] STOE & Cie (1999), X-RED, Version 1.18, STOE & Cie GmbH, Darmstadt, Germany.
[13] G.M. Sheldrick, Acta Crystallogr., Sect. A 46 (1990) 467.
[14] G.M. Sheldrick, SHELXL 97. Program for the Solution and Refinement of Crystal Structures, University of Göttingen, Germany, 1997.
[15] G.M. Sheldrick, SHELXTL: release 4.1 for Siemens Crystallographic Research Systems, 1990.
[16] M.J. Frisch, G.W. Trucks, H.B. Schlegel, G.E. Scuseria, M.A. Robb, J.R. Cheeseman, J.A. Montgomery Jr., T. Vreven, K.N. Kudin, J.C. Burant, J.M. Millam, S.S. Iyengar, J. Tomasi, V. Barone, B. Mennucci, M. Cossi, G. Scalmani, N. Rega, G.A. Petersson, H. Nakatsuji, M. Hada, M. Ehara, K. Toyota, R. Fukuda, J. Hasegawa, M. Ishida, T. Nakajima, Y. Honda, O. Kitao, H. Nakai, M. Klene, X. Li, J.E. Knox, H.P. Hratchian, J.B. Cross, C. Adamo, J. Jaramillo, R. Gomperts, R.E. Stratmann, O. Yazyev, A.J. Austin, R. Cammi, C. Pomelli, J.W. Ochterski, P.Y. Ayala, K. Morokuma, G.A. Voth, P. Salvador, J.J. Dannenberg, V.G. Zakrzewski, S. Dapprich, A.D. Daniels, M.C. Strain, O. Farkas, D.K. Malick, A.D. Rabuck, K. Raghavachari, J.B. Foresman, J.V. Ortiz, Q. Cui, A.G. Baboul, S. Clifford, J. Cioslowski, B.B. Stefanov, G. Liu, A. Liashenko, P. Piskorz, I. Komaromi, R.L. Martin, D.J. Fox, T. Keith, M.A. Al-Laham, C.Y. Peng, A. Nanayakkara, M. Challacombe, P.M.W. Gill, B. Johnson, W. Chen, M. W. Wong, C. Gonzalez, J.A. Pople, GAUSSIAN 03, Revision B.03, Gaussian, Inc., Pittsburgh, PA, 2003.
[17] A.D. Becke, J. Chem. Phys. 98 (1993) 5648.
[18] C. Lee, W. Yang, R.G. Parr, Phys. Rev. B 37 (1988) 785.
[19] M.E. Casida, in: J.M. Seminario (Ed.), Recent Developments and Applications in Modern Density Functional Theory, Theoretical and Computational Chemistry, vol. 4, Elsevier, Amsterdam, 1996.
[20] P.J. Hay, W.R. Wadt, J. Chem. Phys. 82 (1985) 299.
[21] J.L. Lock, G. Turner, Can. J. Chem. 56 (1978) 179.
[22] G. Backes-Dahmann, J.H. Enemark, Inorg. Chem. 26 (1987) 3960.
[23] M. Cano, J.V. Heras, M. Maeso, M. Alvaro, R. Fernández, E. Pinilla, J.A. Campo, A. Monge, J. Organometal. Chem. 534 (1997) 159.
[24] G.A. Jeffrey, W. Saenger, Hydrogen Bonding in Biological Structures, Springer, New York, 1994.
[25] G.R. Desiraju, T. Steiner, The Weak Hydrogen Bond in Structural Chemistry and Biology, Oxford University Press, Oxford, 1999.
[26] R. Taylor, O. Kennard, J. Am. Chem. Soc. 104 (1982) 5063.
[27] J.E. Fergusson, Coord. Chem. Rev. 1 (1966) 459.
[28] A. Earnshaw, B.N. Figgis, J. Lewis, R.D. Peacock, J. Chem. Soc. (1961) 3132.
[29] S. Hirata, M. Head-Gordon, Chem. Phys. Lett. 302 (1999) 375.
[30] R. Andreu, J. Orduna, J. Garín, Tetrahedron 57 (2001) 1358.
[31] E. Brocławik, T. Borowski, Chem. Phys. Lett. 339 (2001) 433.
[32] M.J. Calhorda, M.G.B. Drew, V. Félix, L.P. Fonseca, C.A. Gamelas, S.S.M.C. Godinho, I.S. Gonçavles, E. Hunstock, J.P. Lopes, A.J. Parola, F. Pina, C.C. Romão, A.G. Santos, J. Organomet. Chem. 632 (2001) 94.
[33] A. Crespo, A.G. Turjanski, D.A. Estrin, Chem. Phys. Lett. 365 (2002) 15.
[34] M.C. Aragoni, M. Arca, T. Cassano, C. Denotti, F.A. Devillanova, F. Isaia, V. Lippolis, D. Natali, L. Niti, M. Sampietro, R. Tommasi, G. Verani, Inorg. Chem. Commun. 5 (2002) 869.
[35] P. Romaniello, F. Lelj, Chem. Phys. Lett. 372 (2003) 51.
[36] P. Norman, P. Cronstrand, J. Ericsson, Chem. Phys. 285 (2002) 207.
[37] J. Bossert, N.B. Amor, A. Strich, C. Daniel, Chem. Phys. Lett. 342 (2001) 617.
[38] C.E. Powell, M.P. Cifuentes, A.M. McDonagh, S.K. Hurst, N.T. Lucas, C.D. Delfs, R. Stranger, M.G. Humphrey, S. Houbrechts, I. Asselberghs, A. Persoons, D.C.R. Hockless, Inorg. Chim. Acta 352 (2003) 9.
[39] J.P. Morral, C.E. Powell, R. Stranger, M.P. Cifuentes, M.G. Humphrey, G.A. Heath, J. Organomet. Chem. 670 (2003) 248.
[40] P. Romaniello, F. Lelj, J. Mol. Struct. Theochem. 636 (2003) 23.
[41] B. Machura, M. Jaworska, R. Kruszynski, Inorg. Chem. Commun. (submitted).